ACS chemical biology

Articles

pubs.acs.org/acschemicalbiology

Exploring a 2-Naphthoic Acid Template for the Structure-Based Design of P2Y$_{14}$ Receptor Antagonist Molecular Probes

Evgeny Kiselev,[†] Matthew O. Barrett,[‡] Vsevolod Katritch,[∥] Silvia Paoletta,[†] Clarissa D. Weitzer,[‡] Kyle A. Brown,[‡] Eva Hammes,[†] Andrew L. Yin,[†] Qiang Zhao,[§] Raymond C. Stevens,[∥] T. Kendall Harden,[‡] and Kenneth A. Jacobson*[,†]

[†]Molecular Recognition Section, Laboratory of Bioorganic Chemistry, National Institute of Diabetes and Digestive and Kidney Diseases, National Institutes of Health, Bethesda, Maryland 20892, United States

[‡]Department of Pharmacology, University of North Carolina, School of Medicine, Chapel Hill, North Carolina 27599, United States

[§]CAS Key Laboratory of Receptor Research, Shanghai Institute of Materia Medica, Chinese Academy of Sciences, 555 Zuchongzhi Road, Pudong, Shanghai 201203, China

[∥]Department of Integrative Structural and Computational Biology, The Scripps Research Institute, 10550 North Torrey Pines Road, La Jolla, California 92037, United States

Supporting Information

ABSTRACT: The P2Y$_{14}$ receptor (P2Y$_{14}$R), one of eight P2Y G protein-coupled receptors (GPCR), is involved in inflammatory, endocrine, and hypoxic processes and is an attractive pharmaceutical target. The goal of this research is to develop high-affinity P2Y$_{14}$R fluorescent probes based on the potent and highly selective antagonist 4-(4-(piperidin-4-yl)-phenyl)-7-(4-(trifluoromethyl)-phenyl)-2-naphthoic acid (**6**, PPTN). A model of hP2Y$_{14}$R based on recent hP2Y$_{12}$R X-ray structures together with simulated antagonist docking suggested that the piperidine ring is suitable for fluorophore conjugation while preserving affinity. Chain-elongated alkynyl or amino derivatives of **6** for click or amide coupling were synthesized, and their antagonist activities were measured in hP2Y$_{14}$R-expressing CHO cells. Moreover, a new Alexa Fluor 488 (AF488) containing derivative **30** (MRS4174, K_i = 80 pM) exhibited exceptionally high affinity, as compared to 13 nM for the alkyne precursor **22**. A flow cytometry assay employing **30** as a fluorescent probe was used to quantify specific binding to P2Y$_{14}$R. Known P2Y receptor ligands inhibited binding of **30** with properties consistent with their previously established receptor selectivities and affinities. These results illustrate that potency in this series of 2-naphthoic acid derivatives can be preserved by chain functionalization, leading to highly potent fluorescent molecular probes for P2Y$_{14}$R. Such conjugates will be useful tools in expanding the SAR of this receptor, which still lacks chemical diversity in its collective ligands. This approach demonstrates the predictive power of GPCR homology modeling and the relevance of newly determined X-ray structures to GPCR medicinal chemistry.

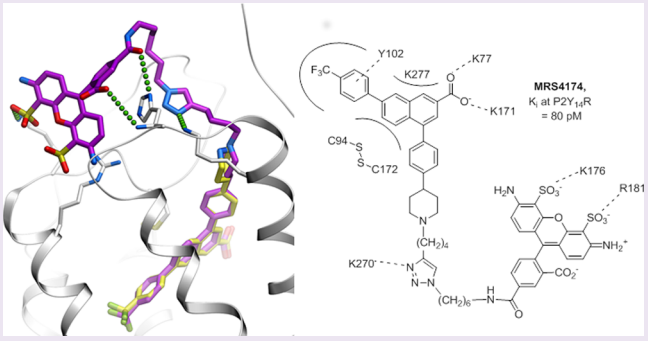

G protein-coupled receptors (GPCRs) are important cell surface signaling proteins with characteristic seven membrane-spanning (7TM) helices. Eight GPCRs that respond to extracellular nucleotides comprise two subfamilies of P2Y receptors based on sequence and functional similarity: P2Y$_1$ receptor (P2Y$_1$R)-like P2Y$_{1,2,4,6,11}$ and P2Y$_{12}$R-like P2Y$_{12-14}$. The cognate agonists of the human (h) P2Y receptors include ADP (P2Y$_1$, P2Y$_{12}$, P2Y$_{13}$), ATP (P2Y$_2$, P2Y$_{11}$), uridine-5′-diphosphate **1** (UDP: P2Y$_6$, P2Y$_{14}$), UTP (P2Y$_2$, P2Y$_4$), and uridine-5′-diphosphoglucose **2** (UDPG: P2Y$_{14}$) (Chart 1).[1] P2Y receptors are widely distributed, with marked expression in a number of tissues including the central and peripheral nervous systems, lung, kidney, intestine, spleen, platelets, and immune cells.[1]

The P2Y$_{14}$R is expressed on immune and epithelial cells and is involved in inflammation and hypoxic processes.[2] Activation of P2Y$_{14}$R contributes to mechanical pain hypersensitivity via microglial cells,[3] enhances the mobility of neutrophils,[4] and promotes the release of mediators from mast cells.[5] Recent studies with P2Y$_{14}$R knockout mice demonstrate the value of P2Y$_{14}$R antagonism as a potential therapeutic goal for diabetes treatment.[6]

Development of selective and potent agonists and antagonists of P2Y$_{14}$R is a highly important goal given the role of this signaling protein in health and disease. To date, the structure–

Received: August 1, 2014
Accepted: October 9, 2014
Published: October 9, 2014

Chart 1. Representative $P2Y_{14}R$ Agonists (1−5) and Antagonists (6−8)

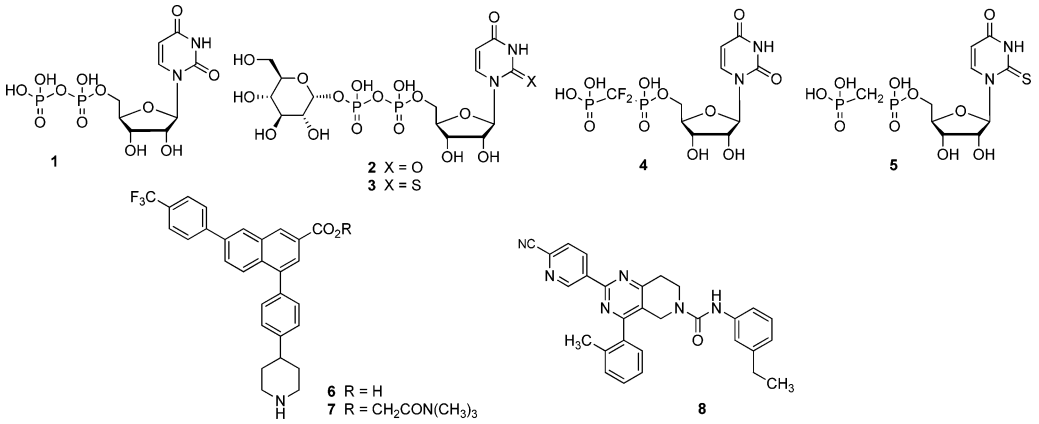

activity relationships (SARs) of only three chemical classes have been extensively evaluated at the $P2Y_{14}R$. The first class consists of synthetic nucleotide analogues of **2**, including potent agonists **3**−**5** (Chart 1).[7,8] The second class is made up of derivatives of 2-naphthoic acid, notably the highly potent and selective antagonist 4-(4-(piperidin-4-yl)-phenyl)-7-(4-(trifluoromethyl)-phenyl)-2-naphthoic acid **6** and its ester prodrug **7**.[9,10] The third class consists of analogues built on a pyrido[4,3-*d*]pyrimidine scaffold, with compound **8** as one of the most potent members.[11] We have used the recently reported high-resolution crystal structures of the $hP2Y_{12}R$ in complex with an antagonist or full agonist[12,13] to construct homology models of the $hP2Y_{14}R$ for ligand docking. This structural insight, which we show to be consistent with ligand pharmacology, has guided our molecular design process at this closely related receptor on the δ-branch of Family A GPCRs.

Most of the analogues of **2** are poor drug candidates due to their low bioavailability and stability; although they could be used *in vitro*, they are not optimal for *in vivo* or tissue-based assays. Various representative compounds of the 2-naphthoic acid class also display poor drug-like characteristics due to high molecular weight and high lipophilicity.[14] Nevertheless, the chemical stability and high affinity and selectivity of **6** toward $P2Y_{14}R$ over other members of the P2Y family make derivatives of **6** potentially attractive candidates for further development of chemical probes for this receptor.[15] We propose to use the 2-naphthoic acid series to design chain-extended analogues that contain fluorescent and other reporter groups for receptor detection and characterization. Such probes could be used in place of radioligands in pharmaceutical research and drug discovery.

RESULTS AND DISCUSSION

A set of functionalized analogues of **6** was designed and prepared (Schemes 1 and 2) from the key ester intermediate **19**, based on predictions from molecular modeling of modes of receptor binding. The strategy behind the selection of these target compounds is described in the following section. Coupling was accomplished by click coupling of an azide and alkyne by copper-catalyzed [2 + 3] cycloaddition[16] or amide condensation.

Molecular Modeling. To identify an energetically favorable binding pose of **6** and to find an appropriate site for fluorophore conjugation, we performed a series of docking studies using homology models of $P2Y_{14}R$.[12,13] Homology models of $hP2Y_{14}R$ were constructed on the basis of two

Scheme 1. Synthesis of (A) *N*-Alkylethynyl Derivatives of 2-Naphthoic Acid Antagonist 6, (B) ω-Ethynylalkylamido Derivatives of 2-Naphthoic Acid Antagonist 6, (C) Terminal Amino and Protected Amino Derivatives of 2-Naphthoic Acid Antagonist 6, and (D) *N*-Methyl Analogue of 6[a]

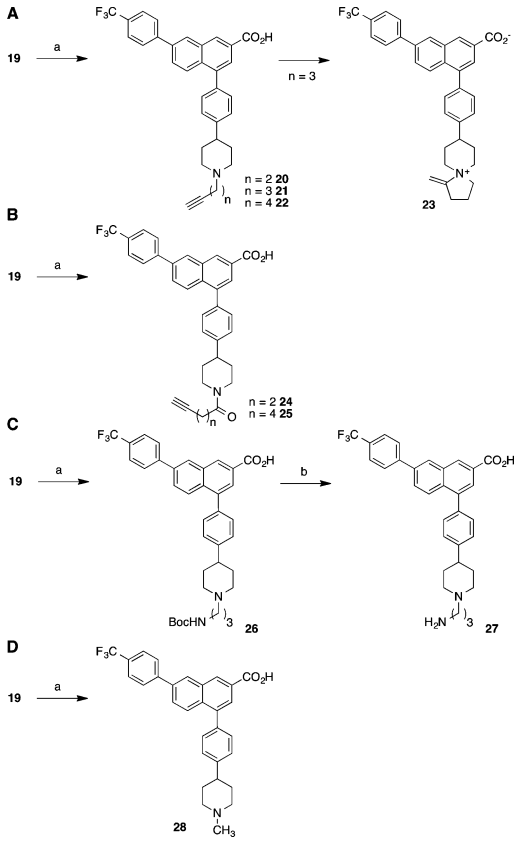

[a]Reagents and conditions for (A): (a) (1) 4-bromobutyne-1 (for **20**), 5-bromopentyne-1 (for **21** and **23**) or 6-bromohexyne-1 (for **22**), K_2CO_3, DMF, 60−70 °C; (2) LiOH (0.5 M), CH_3OH, H_2O (**20**, 46%; **22**, 57%; **23**, 65%). Reagents and conditions for (B): (a) (1) 4-pentynoic acid (for **24**) or 6-heptynoic acid (for **25**), HATU, iPr_2NEt, DMF, 25 °C; (2) LiOH (4 M), CH_3OH, H_2O (**24**, 40%; **25**, 41%). Reagents and conditions for (C): (a) (1) *tert*-butyl (3-bromopropyl)-carbamate, K_2CO_3, DMF, 60−70 °C; (2) LiOH (0.5 M), CH_3OH, H_2O (19%); (b) HCl (3 M), THF, H_2O, 25 °C (26%). Reagents and conditions for (D): (a) CH_2O (aqueous 37%), formic acid, 100 °C; (b) LiOH (0.5 M), CH_3OH, H_2O (55%).

dx.doi.org/10.1021/cb500614p | *ACS Chem. Biol.* 2014, 9, 2833−2842

Scheme 2. Synthesis of Fluorescent Conjugates of the 2-Naphthoic Acid $P2Y_{14}R$ Antagonists[a]

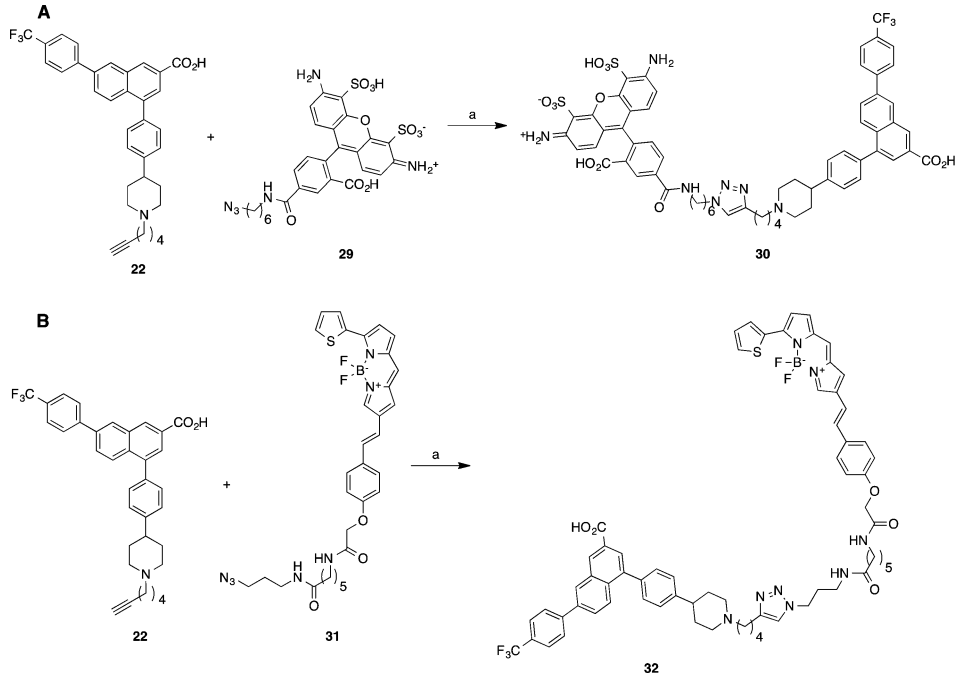

[a](A) AF488 as fluorophore. Reagents and conditions: $CuSO_4$ (7.5% aqueous solution), sodium ascorbate (1 M aqueous solution), *t*BuOH, H_2O, 25 °C (4%). (B) BODIPY as fluorophore. Reagents and conditions: $CuSO_4$, sodium ascorbate, *t*BuOH, H_2O, 25 °C (7.2%).

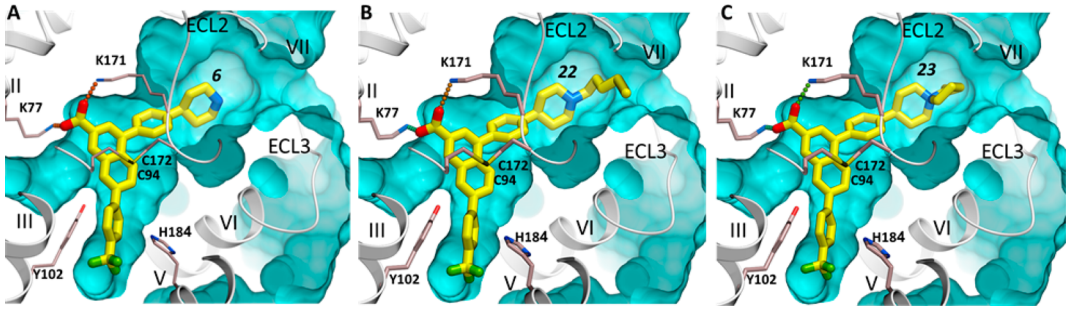

Figure 1. Docking of **6** and its derivatives at the $hP2Y_{14}R$. (A) Predicted binding mode of the original scaffold **6**. (B) Predicted binding mode of hexyne-containing derivative **22**. (C) Predicted binding mode of cyclized azaspiro[4.5]decan-5-ium product **23**. The docked compounds are shown with carbon atoms colored yellow. The $hP2Y_{14}R$ model, shown as gray ribbon and sticks with carbon atoms colored gray, was generated by homology using the $P2Y_{12}R$ crystal structure (PDB ID 4PXZ) and extensive conformational optimization. Ionic interactions of the carboxylic group with lysine side chains are traced as small spheres. The background part of the binding pocket is shown as a cyan surface.

recently solved high-resolution X-ray crystallographic structures of $P2Y_{12}R$,[12,13] which has 49% sequence identity in the 7TM domain to $P2Y_{14}R$. The $P2Y_{12}R$ structure was solved both in complex with the non-nucleotide antagonist ethyl 6-(4-((benzylsulfonyl)carbamoyl)piperidin-1-yl)-5-cyano-2-methylnicotinate (**34**, AZD1283)[17] and with the nucleotide agonist 2-methylthioadenosine 5′-diphosphate (**35**, 2-MeSADP), revealing two very distinct conformational states of the ligand binding pocket.[12,13] Two homology models of $P2Y_{14}R$ based on either an agonist- or antagonist-bound structure of $P2Y_{12}R$ were generated as templates and compared for docking performance.

Docking into the $P2Y_{14}R$ model based on the $P2Y_{12}R$–**34** template did not result in high-score binding poses of the ligand, even when side chain flexibility of the receptor was taken into account. This is likely due to the fact that extracellular loops 1 and 2 (ECL1 and ECL2) are not resolved in the structure of the $P2Y_{12}R$–**34** template, leaving the expected binding pocket widely open and incomplete and rendering the homology model unsuitable for docking new ligands (see Discussion). On the other hand, flexible docking of compound **6** into a $P2Y_{14}R$ model based on the $P2Y_{12}R$–**35** template consistently predicted a high-scoring binding pose in which **6** fits snugly into the narrow cavity and partially overlaps with **35** (Figure 1A). In this pose, the trifluoromethylphenyl moiety of **6** is buried in the hydrophobic pocket closer to the central part of the receptor delineated by residues Val99, Asn156, His184, Ser187, Asn188, and Phe191. The carboxylate group forms an ionic bridge between positively charged amino groups of Lys77 (transmembrane helix 1, TM1) and Lys171 (ECL2) side chains. Most importantly, the 4-piperidylphenyl moiety of **6** in this model points toward the extracellular opening of the pocket so that its charged piperidine group is accessible to solvent. Hence, we concluded that the piperidine nitrogen in **6** is the most suitable location for attaching an elongated chain to link a fluorophore or other reporter group or pharmacophore. Figure 1B depicts one docked alkylated

dx.doi.org/10.1021/cb500614p | *ACS Chem. Biol.* 2014, 9, 2833–2842

analogue of **6** (hexynyl derivative **22** shown in Figure 1 to bind with moderately high $P2Y_{14}R$ affinity) as an illustration of this concept.

The involvement of the carboxylate of **6** in strong polar interactions within the binding site is consistent with known SAR in this series: The inactivity of ester prodrug **7** and its congeners is indicative of the need for a free carboxylate.[14] Thus, it was reported that replacement of the carboxylate functionality of **6** with other neutral (e.g., ester, amide) or negatively charged (e.g., acetic acid, phosphate) moieties led to a decrease in antagonist activity.[9,14] The requirement for a free carboxylate excluded that site from consideration as a potential fluorophore conjugation site.

In the $P2Y_{14}R$ agonist series, we have already explored chain functionalization for conjugation to larger carrier moieties with retention or even enhancement of biological activity. In a series of nucleotide-based agonists, conversion of the carboxylate group of **36** (uridine-5′-diphosphoglucuronic acid) to *N*-alkyl amides preserves potency of the agonist.[8] Additionally, conjugation of **36** to polyamidoamine (PAMAM) dendrimers yielded agonists with enhanced potency, depending on the density of pharmacophore substitution of the polymer.[18]

Thus, we sought to apply a functionalized congener approach to antagonists of the $P2Y_{14}R$. Subsequent SAR exploration of the 2-naphthoic acid class of $P2Y_{14}R$ antagonists was performed to find an appropriate fluorophore−pharmacophore linker.

Chemical Synthesis. The key intermediate ethyl ester **19**[10,14] containing a free piperidine nitrogen was prepared from protected amine **18** as previously described (Supporting Information Scheme 1).[14,15]

Intermediate **14** containing the naphthoic acid core was prepared in four steps from **9** and **10** (Supporting Information Scheme 1).[19] In short, condensation between **9** and **10** in the presence of sodium hydride yielded (*E*)-benzylidenesuccinate **11**. The tertiary butyl ester of **11** was saponified, and the resulting acid **12** was cyclized in the presence of acetic anhydride. Acetate **13** was further hydrolyzed to provide **14**.

The aryl substituents at the naphthoate present in the structures of **6** and **19** were introduced via two consecutive Suzuki transformations in a way similar to that previously described (Supporting Information Scheme 1).[10,15] The Suzuki coupling between **14** and *p*-trifluoromethylphenylboronic acid afforded **15**. Phenol **15** was treated with triflic anhydride followed by bis(pinacolato)diboron to obtain boronate **17**. The second Suzuki reaction between **17** and *tert*-butyl 4-(4-bromophenyl)-5,6-dihydropyridine-1(2*H*)-carboxylate resulted in compound **18**, which contains the framework of **6**. Hydrogenation of **18** followed by carbamate cleavage afforded desired compound **19**.[14]

We began derivatization of **6** by alkylating the piperidine moiety of **19** (Scheme 1). Three homologous alkyl bromides bearing a terminal acetylene group were prepared from the corresponding alcohols[20−23] and used in alkylation to prepare **20**−**22**. It is interesting to note that the product of alkylation of **19** with 5-bromopent-1-yne, i.e., **21**, was not isolated. Instead, a product identified as possessing the structure of **23** was obtained. The structural assignment in the case of cyclized 5-azaspiro[4.5]decan-5-ium product **23** was made on the basis of the ^1H NMR spectra (Supporting Information). This cyclization was observed only during the attempted preparation of precursor **21**, containing three methylene groups adjacent to the alkyne. The characteristic signal from the alkyne proton that would be expected in the case of **21** was absent in the proton NMR spectra. Additionally, two signals were found at 5.61 and 5.93 ppm, respectively, which are consistent with a 2-methylenepyrrolidinium fragment in the context of the structure.[24,25]

Acylated analogues **24** and **25** were prepared through standard amide coupling reactions of **19** with 4-pentynoic and 6-heptynoic acids, respectively, followed by the hydrolysis of the ethyl ester with lithium hydroxide (Scheme 2).

Two additional *N*-alkyl analogues **26** and **27** were prepared via alkylating **19** with *tert*-butyl (3-bromopropyl)carbamate[26] followed by ester hydrolysis and carbamate cleavage. Analogue **27** contains an amino group that could be used to attach a fluorophore through acylation reactions. Compound **26** was included in the set of compounds as a test of how a bulky group such as *tert*-butyloxycarbonyl (Boc) or potentially a fluorophore would be tolerated in binding to the receptor.

The longest of the alkyne intermediates, **22**, containing four methylene groups, was further treated with AF488 azide **29** containing a widely used fluorophore to furnish **30** as a fluorescent analogue of **6** (Scheme 2A). Similarly, analogue **32** was prepared by treating **22** with azide **31** carrying a boron-dipyrromethene (BODIPY) fluorescent moiety (Scheme 2B), which was prepared as reported.[27] Compound **22** was chosen for further modification based on the observed hypothetical binding mode: the longer hexynyl chain reaches closer to the extracellular entrance to the binding pocket between ECL3 and helix VII (TM7, Figure 1B). We hypothesized that placing the alkyne at the entrance of the pocket, distal from the core pharmacophore binding site, would reduce the steric interference with ligand binding when conjugated to the fluorophore. The excitation and emission spectra of **30** and **32** show the expected maxima (**30**, 496 and 519 nm, respectively; **32**, 626 and 642 nm, respectively) for these fluorophores (Supporting Information).

Biological Characterization. All synthetic analogues were evaluated functionally in Chinese hamster ovary (CHO) cells stably expressing $hP2Y_{14}R$ ($P2Y_{14}R$-CHO cells, Table 1).[15] The activity of each antagonist analogue at the $P2Y_{14}R$ was quantified by measuring its capacity to antagonize the agonist action of the native agonist uridine-5′-diphosphoglucose **2**. Thus, **2**-promoted inhibition of cyclic AMP accumulation was measured in the presence of an EC_{80} concentration (316 nM)

Table 1. Functional Evaluation of Antagonism by the 2-Naphthoic Acid Analogues in CHO Cells Stably Expressing $hP2Y_{14}R$[a]

compd	K_i (nM)
6	0.3 ± 0.1
19	120 ± 8
20	2.7 ± 1.2
22	13.0 ± 1.1
23	2.0 ± 0.2
24	6.7 ± 2.2
25	8.3 ± 1.9
26	26.0 ± 6.0
27	14.0 ± 2.4
28	7.1 ± 1.6
30	0.08 ± 0.02
32	>100

[a]Antagonism of the inhibition of cyclic AMP accumulation induced by **2** (316 nM) acting at the $hP2Y_{14}R$ in the presence of 30 μM forskolin.

dx.doi.org/10.1021/cb500614p | *ACS Chem. Biol.* 2014, 9, 2833−2842

of **2** alone or in the presence of 316 nM **2** and increasing concentrations (half-log concentrations between 10^{-10} and 10^{-5} M) of each newly synthesized molecule. IC_{50} values for **20** and **22**–**27** were determined from these inhibition curves, and K_i values were calculated using the Cheng–Prusoff equation.[28]

$P2Y_{14}R$ antagonistic activities for the *N*-substituted analogues of **6** remained in the low nanomolar range. The order of potency for these derivatives was as follows: short alkyne **20**, cyclized **23** > *N*-acylpiperidines **24**, **25** > long alkyne **22**, aminopropyl derivative **27** > Boc-aminopropyl derivative **26**. Ethyl ester **19** was 400-fold weaker as an antagonist than that of free carboxylate analogue **6**. This confirms the tentative conclusion based on published work that the carboxylate is important for recognition of the 2-naphthoic acid series of $P2Y_{14}R$ antagonists.[9,14] *N*-Methyl derivative **28** displayed significant receptor affinity, emphasizing that the NH of the piperidine ring of **6** is not required for interaction with the $P2Y_{14}R$ and that this N is a suitable site for chain extension.

The high affinity of the cyclized azaspiro[4.5]decan-5-ium product **23** (K_i 2.0 nM) suggests some tolerance of steric bulk in that region. Because the amino group of the piperidine moiety of **23** is quaternized, it does not participate in direct H-bonding with the receptor. Docking of this compound to $P2Y_{14}R$ confirmed that the predicted orientation of the naphthoic acid scaffold can easily accommodate a rigid spiro ring (Figure 1C).

AF488 derivative **30** displayed enhanced potency as an antagonist with a K_i of 80 pM, compared to 0.3 nM for **6** and 13 nM for hexynyl intermediate **22** (Figure 2). In comparison, BODIPY derivative **32** was much weaker in its interaction with $P2Y_{14}R$. Thus, **30** was identified as a very promising candidate fluorescent probe of $P2Y_{14}R$.

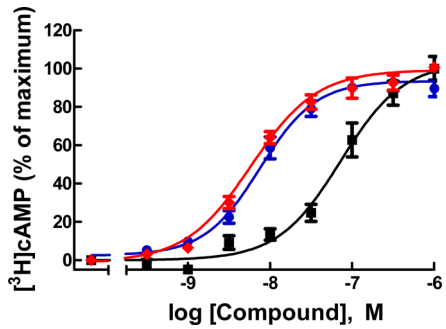

Figure 2. Concentration–response curves for **6** (blue), alkyne **22** (black), and conjugate **30** (red) in antagonism of the inhibition of cAMP formation via human $P2Y_{14}R$ in $P2Y_{14}R$-CHO cells.

AF488 conjugate **30** bound specifically to the receptor in intact $P2Y_{14}R$-CHO cells, as characterized using flow cytometry (FCM), a technique previously used in intact cell studies with fluorescent antagonists of other GPCRs.[29] Cell labeling using the fluorescent probe at a fixed concentration of 10 nM was compared at two different incubation times; the level of specific binding of **30** was greater following a 30 min incubation compared to that at 20 min (Figure 3). A 30 min preincubation with agonists **1**, **3**, or **36** at 10 μM or antagonist **6** at 10 μM largely prevented the labeling in $P2Y_{14}R$-CHO cells. The high fraction of specific binding of **30** is evident in Figure 4, which compares total cell fluorescence with exposure to various combinations of ligands. The residual nonspecific binding in the presence of 10 μM **6** is only 1.9% (20 min) or 1.1% (30 min) of the total binding of 10 nM **30** (Figure 4). Both a $P2Y_1R$ selective antagonist N^6-methyl-2′-deoxyadenosine-3′,5′-bisphosphate (**37**, MRS2179)[38] and a $P2Y_6R$ selective irreversibly binding antagonist *N*,*N*″-1,4-butanediyl*bis*[*N*′-(3-isothiocyanatophenyl)]thiourea (**38**, MRS 2578) failed at 10 μM to prevent binding of **30**. A weak, nonselective P2R antagonist suramin (at 10 μM) demonstrated only a minor reduction of the level of fluorescent cell labeling. The efficiency of inhibition of fluorescent labeling by competing ligands was in the order **6** > **3** > **1** (Figure 4), corresponding to their order of apparent affinities at the $P2Y_{14}R$.[8,15]

Use of the BODIPY conjugate **32** was compared to **30** in experiments applying FCM. Although labeling of live $P2Y_{14}R$-CHO cells by **32** was inhibited following preincubation with known $P2Y_{14}R$ ligands, it displayed significant nonspecific binding in control CHO cells, which increased upon prolonged incubation (Figure 3F). Thus, AF488 conjugate **30** had more desirable characteristics than **32** as a tracer for receptor detection and characterization and potentially in drug screening for activity at the $P2Y_{14}R$.

The predicted binding mode of **30** in the $P2Y_{14}R$, as characterized by the best conformational energy of the complex, is presented in Figure 5. Note that despite full flexibility of the ligand and the receptor pocket side chains the docking pose of the 2-naphthoic acid scaffold is almost identical to the one observed for **6**, suggesting well-defined tight binding of this chemical scaffold. Beyond this scaffold, the triazole ring of the linker region of compound **30** interacts with the receptor through a salt bridge to the side chain of Lys270, which may contribute to the unusually high affinity of **30**. Other interactions contributing to the binding affinity of **30** may be mediated by the AF488 moiety itself. Thus, the fluorophore moiety is predicted to reach back into the shallow groove in the ECL region of the receptor, where its carbonyl and carboxyl moieties make polar interactions with the side chain and main chain nitrogens of His264. One of its sulfonate groups also forms a salt bridge to the primary amine of Lys176. Such interactions of the AF488 substitution are unlikely to be strong or highly specific. Nonetheless, they favorably contribute to the binding of **30** and explain the 4-fold increase in affinity compared to that of **6** and the 160-fold increase compared to that of **22**, which is the closest precursor of **30** studied here.

In general, additional ligand tools and molecular probes are needed for characterizing and defining the action of P2YRs.[38] Few radioligands for this family of receptors exist, and only a few subtypes can be targeted with selective agonists and/or antagonists.

This work is directed toward development of molecular probes for $P2Y_{14}R$ that are structurally derived from a newly reported potent and highly selective antagonist **6**. In the absence of an atomic resolution structure of $P2Y_{14}R$, we constructed homology models based on recently reported structures of the closely related $P2Y_{12}R$[12,13] and used them for virtual docking of $P2Y_{14}R$-directed antagonists. Application of these models resulted in identification of the piperidine ring as a likely site for chain derivatization with preservation of affinity, and a series of analogues was synthesized to probe the effect of distal changes on antagonist potency. The structure of the $P2Y_{12}R$ template was recently solved both in complex with a non-nucleotide antagonist **34** and with the nucleotide agonist **35**, revealing drastically different conformations of the receptor.[12,13] The $P2Y_{12}R$–**34** antagonist complex structure (PDB ID 4NTJ) revealed a wide open binding pocket due to

dx.doi.org/10.1021/cb500614p | *ACS Chem. Biol.* 2014, 9, 2833–2842

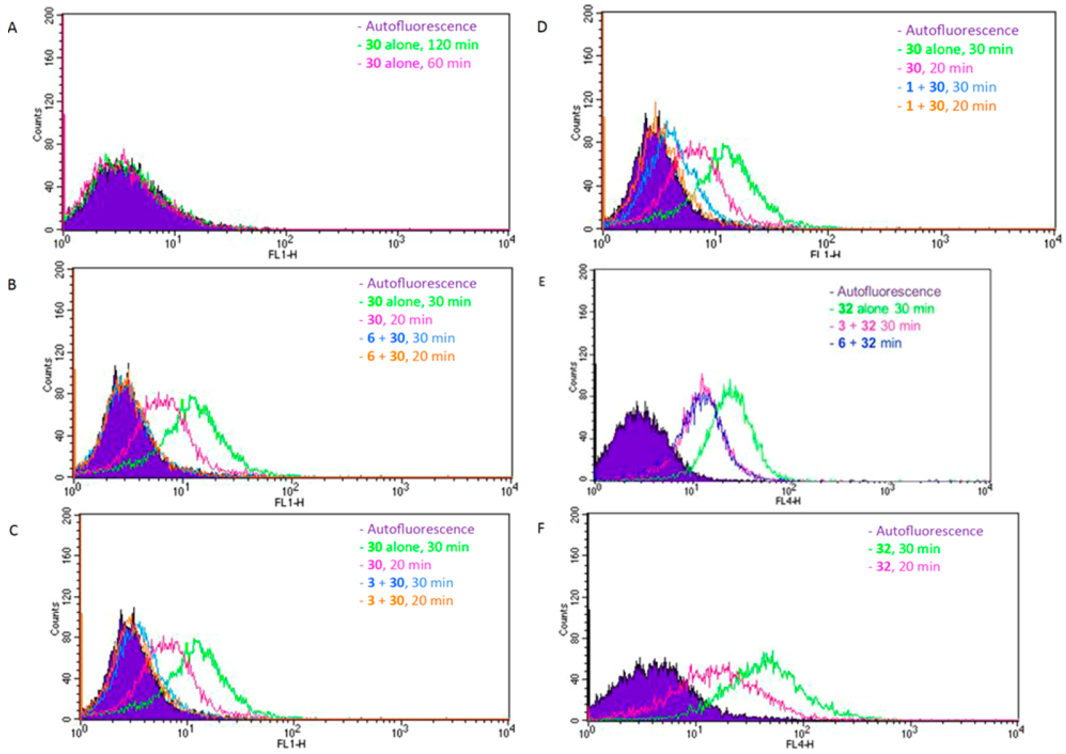

Figure 3. Binding of Alexa Fluor 488 (AF488) conjugate **30** (A–D) and boron-dipyrromethene (BODIPY) conjugate **32** (E, F) at the hP2Y$_{14}$R as characterized using FCM. Fluorescent ligands were present at 10 nM, and preincubation with competing ligands was for 30 min at 37 °C. (A) Lack of nonspecific binding in control CHO cells of fluorescent antagonist **30**. (B) Binding in P2Y$_{14}$R-expressing CHO cells of fluorescent antagonist **30** alone or after preincubation with competing antagonist **6** (10 μM). (C) Binding in P2Y$_{14}$R-expressing CHO cells of fluorescent agonist **30** alone or after preincubation with competing agonist **3** (5 μM). (D) Binding in P2Y$_{14}$R-expressing CHO cells of fluorescent antagonist **30** alone or after preincubation with competing native agonist **1** (10 μM). (E) Binding in P2Y$_{14}$R-expressing CHO cells of fluorescent antagonist **32** alone or after preincubation with competing agonists **3** and antagonist **6** (all, 10 μM). (F) Nonspecific binding in control CHO cells of fluorescent antagonist **32**.

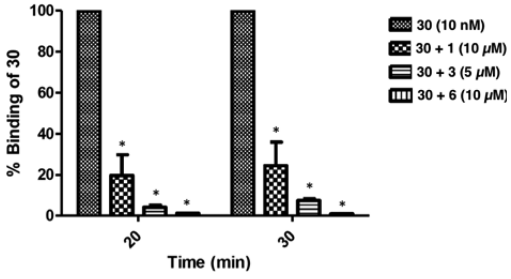

Figure 4. Fluorescence ligand binding experiments using flowcytometry (FCM) in P2Y$_{14}$R-CHO cells with **30** after 30 min preincubation at 37 °C with known P2Y$_{14}$R agonists **1** and **3** or P2Y$_{14}$R antagonist **6**. Each column shows the brightness of each compound using **30** normalized to 100% for each time point and after correcting the mean fluorescence intensity values for autofluorescence. Results at 30 min expressed as mean ± SEM (n = 4) are 24.4 ± 11.5%, **1**; 7.5 ± 0.8%, **3**; 1.10 ± 0.06%, **6**. *, P < 0.05, when compared to cells treated with only **30**. No significant difference in mean fluorescence intensity was observed at 30 min in the presence of P2Y$_1$R antagonist **37** (10 μM, 80.9 ± 8.6%, data not shown) or P2Y$_6$R antagonist **38** (10 μM, 100.7 ± 10.5%, data not shown). Fluorescence in the presence of weak, nonselective P2R antagonist suramin (10 μM) was 82.1 ± 3.6% (data not shown).

the unresolved ECL1 and ECL2 regions and the outward positions of helices VI (TM6) and VII (TM7). In contrast, TM6/TM7 are shifted toward the ligand in the agonist-bound P2Y$_{12}$R structure (PDB ID 4PXZ), and the extracellular loops form a "lid" on top of ligand binding site participating in ligand coordination.

Our modeling and docking results suggested that the closed conformation of the extracellular region of P2Y$_{14}$R is more suitable for binding compound **6**, providing a reasonable steric fit for this high-affinity antagonist. The trifluoromethylphenyl group is bound within the largely hydrophobic subpocket, forming a $\pi-\pi$ interaction with the Tyr102 side chain (a $\pi-\pi$ interaction with ligands was found in all X-ray structures of P2Y$_{12}$R). The carboxylate group forms strong charge−charge interactions with the positively charged side chains of Lys77 and Lys171, and the piperidinyl-phenyl moiety is sandwiched between TM7 and ECL2, with the piperidine nitrogen directed toward the extracellular side of the receptor. In contrast, the model based on the P2Y$_{12}$R−**34** template was not efficient in docking compound **6** or its derivatives, as it did not yield any high-scoring binding conformations. A possible explanation of this result is that the disordered conformational state of the extracellular region is specific to the P2Y$_{12}$R complex with **34**, an antagonist that apparently pushes TM6 outward and precludes a closed conformation of the loops.[12] Moreover, our analysis suggests that some features of the extracellular region of the P2Y$_{14}$R may favor a closed conformation of ECL2. Thus, despite high sequence similarity and gapless alignment between P2Y$_{12}$R and P2Y$_{14}$R (Supporting Information Figure 1), the ECL2 residues in P2Y$_{14}$R carry only minimal electrostatic charge (+1) compared to the highly charged ECL2 in P2Y$_{12}$R (+5 charge within a 15 residue stretch of this loop). While the excessive positive charge of ECL2 in the

dx.doi.org/10.1021/cb500614p | ACS Chem. Biol. 2014, 9, 2833−2842

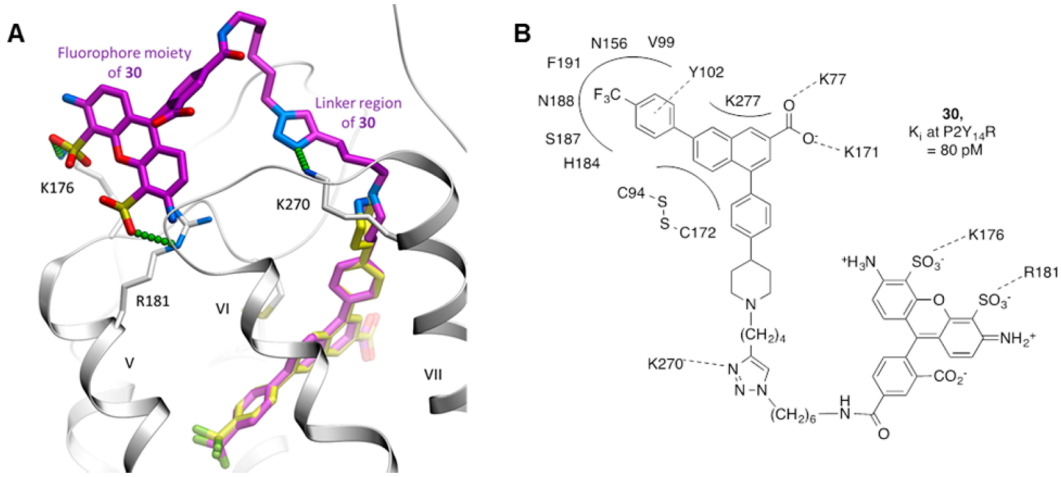

Figure 5. Predicted binding of compound **30** at the hP2Y$_{14}$R. Compound **30** is shown as sticks with carbon atoms colored magenta. For comparison, the original scaffold **6** (the same conformation as in Figure 1A) is shown with carbon atoms colored light yellow. Predicted polar and ionic interactions of the triazole and AF488 fluorophore moieties of **30** with the receptor are traced by small green spheres. hP2Y$_{14}$R is shown as a ribbon and sticks with carbon atoms colored gray.

P2Y$_{12}$R is thought to destabilize the loop in the absence of ATP/ADP analogues, the more neutral ECL2 in P2Y$_{14}$R may favor the closed conformation even in an antagonist-bound or apo state. Predicted binding of compound **6** may further stabilize ECL2, since its carboxylate group forms ionic bridges with both Lys77 in TM2 and Lys171 in ECL2 in an extensive network of ionic interactions that also involves Lys277, Arg274, Asp81, and Glu278 (Supporting Information Figure 2). Our modeling therefore suggests novel insight into conformational states of the P2Y$_{14}$R that are more reminiscent of the closed, rather than the open conformational state observed in the crystal structure of P2Y$_{12}$R.

The placement of the piperidine moiety of docked **6** in a solvent-accessible pocket within the receptor initially led us to hypothesize that preservation of the protonated and charged state of this group might be important for retaining the affinity of target molecules for P2Y$_{14}$R. However, biological characterization of the analogues synthesized revealed no advantage in potency for *N*-alkylated analogues of **6** in comparison tothat of *N*-acylated derivatives.

A goal of this research is to introduce reliable probes for P2Y$_{14}$R to provide methods for fluorescent characterization of P2Y$_{14}$R both in membranes and intact cells. The derivatives of **6** were furnished with alkynyl or amino groups, suitable for attachment of fluorescent moieties by click chemistry or amide coupling, respectively. Compounds **20**, **22**, **26**, and **27** displayed potencies within an order of magnitude of that of the parent molecule **6**, and these may be suitable for further conjugation with fluorescent dyes. Thus, our results demonstrate that P2Y$_{14}$R potency can be preserved by chain functionalization, leading to fluorescent molecular probes for the receptor. Fluorescent ligands were reported previously for other P2YRs (P2Y$_{2,4,6}$), but these are nucleotide agonist analogues that are subject to agonist-promoted internalization.[27,30] Compound **30** is the first fluorescent antagonist probe of high affinity for a P2YR. It combines a hydrophilic fluorophore with a hydrophobic pharmacophore and consequently exhibits low nonspecific binding. The charged groups on the AF488 moiety are predicted to interact with charged amino acid residues on the ELs of the receptor to stabilize the high-affinity complex. It is likely that distal interactions on the ELs contribute to the exceptionally high affinity (80 pM) of **30**. In contrast, BODIPY conjugate **32** is much more hydrophobic and displayed an unacceptable level of nonspecific binding in control CHO cells and a low affinity at the P2Y$_{14}$R. More promising analogues now can be applied to the study of tissues and cells in disease models such as human neutrophils, where P2Y$_{14}$R promotes chemotaxis,[4] or in LAD2 human mast cells, where the receptor promotes release of inflammatory mediators.[5] In addition to well-described agonist-mediated GPCR internalization, there are reports of antagonist-induced internalization.[39] Fortunately, no such internalization has been observed in the FCM experiments (Figures 3A,B and 4). It could be seen that with incubation in the presence of parent antagonist **6** there is near complete reversal of binding of **30** (Figures 3B and 4), excluding the possibility of fluorescence uptake through receptor internalization in the time frame of the experiment. Additionally, the incubation of **30** with CHO cells lacking expression of P2Y$_{14}$R for up to 2 h has shown no significant nonspecific binding (Figure 3A), thus excluding the possibility of passive transport of **30** through the membrane.

In conclusion, we used molecular modeling based on a closely related structural template of P2Y$_{14}$R to identify the piperidine moiety of **6** as the most structurally permissive region of the antagonist for derivatization, with the objective of covalent chain attachment through a tertiary amino group. The pharmacological results for the newly synthesized compound series were consistent with the structural insights gained from P2Y$_{12}$R-based homology modeling and docking at this closely related receptor. The resulting P2Y$_{14}$R model with its ECLs defined conformationally allows prediction of specific interactions with antagonist analogues. This approach demonstrates the predictive power of GPCR homology modeling and the value of applying newly determined X-ray structures to the medicinal chemistry of GPCRs. Our results indicate that P2Y$_{14}$R potency in this series of 2-naphthoic acid derivatives can be preserved by chain functionalization, leading to selective fluorescent molecular probes for the receptor. Indeed, AF488 conjugate **30** displayed highly favorable properties when used as a tracer in whole-cell binding assays of P2Y$_{14}$R using FCM: pharmacological selectivities consistent with the apparent affinities of known P2Y ligands, unusually high receptor affinity

dx.doi.org/10.1021/cb500614p | *ACS Chem. Biol.* 2014, 9, 2833−2842

of the tracer, and strikingly low nonspecific binding. The measurement of precise $P2Y_{14}R$ selectivity and *in situ* labeling, kinetics, and receptor saturation by **30** as well as development of routine screening methods will be the subject of future studies. Fluorescent ligand probes are of increasing interest as pharmacological tools for characterizing GPCRs.[40] Such conjugates will be useful tools in expanding the SAR at this receptor, which still lacks chemical diversity in its collective ligands.

METHODS

Homology Modeling. Homology modeling of $hP2Y_{14}R$ was performed using the recently solved high-resolution crystallographic structures of $hP2Y_{12}R$,[12,13] a closely related member of the P2YR subfamily. Within the 7TM domain portion of the receptor, the alignment between $P2Y_{12}R$ and $P2Y_{14}R$ sequences is fully continuous (gapless), with sequence identity as high as 49%, which facilitated reliable model building. The homology modeling was performed with the ICM-Pro molecular modeling package's build model function using full energy-based conformational sampling and optimization of the side chains in internal coordinates.[31−33] Both the closed conformation of the $hP2Y_{12}R$ extracellular region (PDB ID 4PXZ) and the open conformation (PDB ID 4NTJ) were used to generate the models for the docking procedure.

Docking. Compounds **6**, **22**, and **23** were docked into the models of $hP2Y_{14}R$ using ICM-Pro molecular modeling software.[31] The ligand and residue side chains forming the binding pocket were treated as flexible, and their conformation was thoroughly sampled in 10^6 Monte Carlo (10^7 for compound **30**) optimization steps to global convergence of the physics-based energy function.[34] The docking procedure was repeated in 5 independent runs from different starting positions of the ligand outside of the pocket. Soft van der Waals potentials and a high temperature parameter were used to facilitate ligand sampling. The criteria for docking procedure convergence included a high score for the predicted binding of the ligand in the energy optimized complex (score < −30) and a consistently reproduced docking conformations (RMSD < 1.5 Å). Note that the $hP2Y_{14}R$ model based on the open receptor conformation did not satisfy either of these criteria for docking of small compounds **6**, **22**, and **23** and therefore was not used in docking of a larger compound **30**. Starting positions for docking of compound **30** used optimal docking position of compound **6**, while the position of fluorophore and linker was randomized.

Pharmacological Assays: Cell Culture and Reagents. CHO cells stably expressing $hP2Y_{14}R$ were generated as previously described,[35] grown in F-12 medium with 10% FBS and 1% geneticin, and maintained at 37 °C in 5% CO_2. 3-Isobutyl-1-methylxanthine (IBMX), forskolin, and **2** were purchased from Sigma-Aldrich. [^{3}H]Adenine was purchased from American Radiolabeled Chemicals (St. Louis, MO). Geneticin, serum, and all cell culture medium were purchased from Gibco Life Technologies.

Quantification of Cyclic AMP Accumulation. $P2Y_{14}R$-CHO cells were plated in 24-well plates approximately 24 h before the assay at 70 000 cells per well and were labeled 2 h before the assay with 1 mCi [^{3}H]adenine/well in 25 mM 4-(2-hydroxyethyl)-1-piperazineethanesulfonic acid (HEPES)-buffered serum-free DMEM. All assays were performed in the presence of 200 μM IBMX, a phosphodiesterase inhibitor, and were initiated by the addition of 30 μM forskolin. Tests of the antagonist activities of each of the newly synthesized molecules were carried out using an EC_{80} concentration (316 nM) of $P2Y_{14}R$ agonist **2** and a range of concentrations of the antagonist that usually spanned 5 orders of magnitude. Incubations were for 15 min at 37 °C and were terminated by aspiration of medium and addition of 500 μL of ice-cold 5% trichloroacetic acid. [^{3}H]Cyclic-AMP was isolated by sequential Dowex and alumina chromatography as previously described.[36,37]

Data Analysis. Agonist potencies (EC_{50} values) were obtained from concentration−response curves by nonlinear regression analysis using the GraphPad software package Prism. All experiments were performed in triplicate assays and repeated at least three times. The results are presented as mean ± SEM from multiple experiments or, in the case of concentration−effect curves, from a single experiment carried out with triplicate assays that were representative of results from multiple experiments.

Cell Cultures for FCM. CHO-$P2Y_{14}R$ cells and wild-type CHO cells were grown in DMEM/F12 (1:1) with 10% FBS, 50 U/mL penicillin/streptomycin, and 2 mM L-glutamine. Cells were grown in 6-well plates (approximately 3×10^5 cells/well) and incubated at 37 °C in 5% CO_2. When the cells reached 80% confluence, the medium was replaced with fresh preheated medium. Compound **30** was added in the presence or absence of the appropriate agonist or antagonist of $P2Y_{14}R$, and the decrease in fluorescence intensity was measured by FCM.

Fluorescent Ligand Binding in CHO-$P2Y_{14}R$ Cells. CHO-$P2Y_{14}R$ cells were incubated with known agonists or antagonists of $P2Y_{14}R$, such as agonists **1**, **3**, and **36** or antagonist **6**. The cells were preincubated for 30 min with the known agonist or antagonist at 37 °C in 5% CO_2. Two different incubation times (20 and 30 min) in the presence of fluorescent antagonist **30** were compared.

Following incubation with **30**, the medium was removed, the cells were washed three times with ice-cold DPBS, and 1 mL of 0.2% EDTA was added to each well to detach the cells from the plate. After detaching, 1 mL of medium was added to neutralize the EDTA, and the cell suspension was incubated at 37 °C for 5−10 min. The cell suspensions were transferred to 5 mL polystyrene round-bottomed BD Falcon tubes and centrifuged for 5 min at 23 °C and 400*g*. After the supernatant was discarded, the cells were washed with 3 mL of DPBS and centrifuged again at 23 °C and 400*g* for 5 min. After centrifugation, the supernatant was discarded, and the cells were resuspended in 0.5 mL of DPBS for analysis by FCM.

FCM Analysis. The intensity of fluorescence emission of each sample was measured using FCM. Cell suspensions were vortexed briefly before analysis on a BD FACSCalibur flow cytometer. Samples were maintained in the dark during the analysis to avoid photobleaching. Mean fluorescent intensity was obtained in log mode using the FL-1 channel for **30** and FL-4 channel for **32**, and 10 000 events were analyzed per sample. Data were collected and analyzed using BD Cell Quest Pro software. Data analysis was performed with GraphPad Prism 5 software. The mean autofluorescence of CHO cells was measured in the absence of the fluorescent ligand. The mean fluorescence intensity in the presence of fluorescent ligand was corrected by subtracting the autofluorescence.

ASSOCIATED CONTENT

Supporting Information

Coordinate file of the $P2Y_{14}R$ model complex with **30**; scheme for synthesis of **19**; synthesis procedures used for preparation of **19**, **20**, **22**−**28**, **30**, and **32**; NMR and mass spectra of selected compounds; and fluorescence spectra of **30** and **32**. This material is available free of charge via the Internet at http://pubs.acs.org.

AUTHOR INFORMATION

Corresponding Author

*E-mail: kajacobs@helix.nih.gov.

Notes

The authors declare no competing financial interest.

ACKNOWLEDGMENTS

Mass spectral measurements were carried out by J. Lloyd and N. Whittaker (NIDDK). We acknowledge support from the NIGMS Postdoctoral Research Associate (PRAT) Program and the Intramural Program of the National Institute of Diabetes and Digestive and Kidney Diseases. This work was supported

by National Institutes of Health grant nos. GM38213 to T.K.H. and U54GM094618 to V.K. and R.C.S.

■ ABBREVIATIONS

AF488, Alexa Fluor 488; BODIPY, boron-dipyrromethene; CHO, Chinese hamster ovary; DMEM, Dulbecco's modified Eagle's medium; DMF, dimethylformamide; DPPF, 1,1′-bis(diphenylphosphino)ferrocene; ECL, extracellular loop; EDC, *N*-ethyl-*N*′-dimethylaminopropylcarbodiimide; HATU, 1-[bis(dimethylamino)methylene]-1*H*-1,2,3-triazolo[4,5-*b*]-pyridinium 3-oxid hexafluorophosphate; PLC, phospholipase C; PPTN, 4-(4-(piperidin-4-yl)-phenyl)-7-(4-(trifluoromethyl)-phenyl)-2-naphthoic acid; SAR, structure−activity relationship; UDPG, uridine-5′-diphosphoglucose; THF, tetrahydrofuran; TM, transmembrane helix

■ REFERENCES

(1) Boeynaems, J.-M., Communi, D., and Robaye, B. (2012) Overview of the pharmacology and physiological roles of P2Y receptors. *Wiley Interdiscip. Rev.: Membr. Transp. Signaling 1*, 581−588.

(2) Harden, T. K., Sesma, J. I., Fricks, I. P., Lazarowski, E. R. Signalling and pharmacological properties of the $P2Y_{14}$ receptor. *Acta Physiol. 199*, 149−160.

(3) Kobayashi, K., Yamanaka, H., Yanamoto, F., Okubo, M., and Noguchi, K. (2012) Multiple P2Y subtypes in spinal microglia are involved in neuropathic pain after peripheral nerve injury. *Glia 60*, 1529−1539.

(4) Sesma, J. I., Kreda, S. M., Steinckwich-Besancon, N., Dang, H., García-Mata, R., Harden, T. K., and Lazarowski, E. R. (2012) The UDP-sugar-sensing $P2Y_{14}$ receptor promotes Rho-mediated signaling and chemotaxis in human neutrophils. *Am. J. Physiol.: Cell Physiol. 303*, C490−C498.

(5) Gao, Z.-G., Ding, Y., and Jacobson, K. A. (2010) UDP-glucose acting at $P2Y_{14}$ receptors is a mediator of mast cell degranulation. *Biochem. Pharmacol. 79*, 873−879.

(6) Xu, J., Morinaga, H., Oh, D., Li, P., Chen, A., Talukdar, S., Lazarowski, E., Olefsky, J. M., and Kim, J. J. (2012) GPR105 ablation prevents inflammation and improves insulin sensitivity in mice with diet-induced obesity. *J. Immunol. 189*, 1992−1999.

(7) Ko, H., Fricks, I., Ivanov, A. A., Harden, T. K., and Jacobson, K. A. (2007) Structure−activity relationship of uridine 5′-diphosphoglucose analogues as agonists of the human $P2Y_{14}$ receptor. *J. Med. Chem. 50*, 2030−2039.

(8) Ko, H., Das, A., Carter, R. L., Fricks, I. P., Zhou, Y., Ivanov, A. A., Melman, A., Joshi, B. V., Kováč, P., Hajduch, J., Kirk, K. L., Harden, T. K., and Jacobson, K. A. (2009) Molecular recognition in the $P2Y_{14}$ receptor: probing the structurally permissive terminal sugar moiety of uridine-5′-diphosphoglucose. *Bioorg. Med. Chem. 17*, 5298−5311.

(9) Gauthier, J. Y., Belley, M., Deschênes, D., Fournier, J.-F., Gagné, S., Gareau, Y., Hamel, M., Hénault, M., Hyjazie, H., Kargman, S., Lavallée, G., Levesque, J.-F., Li, L., Mamane, Y., Mancini, J., Morin, N., Mulrooney, E., Robichaud, J., Thérien, M., Tranmer, G., Wang, Z., Wu, J., and Black, W. C. (2011) The identification of 4,7-disubstituted naphthoic acid derivatives as UDP-competitive antagonists of $P2Y_{14}$. *Bioorg. Med. Chem. Lett. 21*, 2836−2839.

(10) Belley, M., Deschenes, D., Fortin, R., Fournier, J.-F., Gagne, S., Gareau, Y., Gauthier, J. Y., Li, L., Robichaud, J., Therien, M., Tranmer, G. K., and Wang, Z. (2009) Substituted 2-naphthoic acids as antagonists of GFPR105 activity. WO2009070873 A1, June 11, 2009.

(11) Guay, D., Beaulieu, C., Belley, M., Crane, S. N., DeLuca, J., Gareau, Y., Hamel, M., Henault, M., Hyjazie, H., Kargman, S., Chan, C. C., Xu, L., Gordon, R., Li, L., Mamane, Y., Morin, N., Mancini, J., Thérien, M., Tranmer, G., Truong, V. L., Wang, Z., and Black, W. C. (2011) Synthesis and SAR of pyrimidine-based, non-nucleotide $P2Y_{14}$ receptor antagonists. *Bioorg. Med. Chem. Lett. 21*, 2832−2835.

(12) Zhang, K., Zhang, J., Gao, Z. G., Zhang, D., Zhu, L., Han, G. W., Moss, S. M., Paoletta, S., Kiselev, E., Lu, W., Fenalti, G., Zhang, W., Müller, C. E., Yang, H., Cherezov, V., Katritch, V., Han, G. W., Jacobson, K. A., Stevens, R. C., Wu, B., and Zhao, Q. (2014) Structure of the human $P2Y_{12}$ receptor in complex with an antithrombotic drug. *Nature 509*, 115−118.

(13) Zhang, K., Zhang, J., Gao, Z. G., Paoletta, S., Zhang, D., Han, G. W., Li, T., Ma, L., Zhang, W., Müller, C. E., Yang, H., Jiang, H., Cherezov, V., Katritch, V., Jacobson, K. A., Stevens, R. C., Wu, B., and Zhao, Q. (2014) Agonist-bound structure of the human $P2Y_{12}$R receptor. *Nature 509*, 119−122.

(14) Robichaud, J., Fournier, J.-F., Gagné, S., Gauthier, J. Y., Hamel, M., Han, Y., Hénault, M., Kargman, S., Levesque, J.-F., Mamane, Y., Mancini, J., Morin, N., Mulrooney, E., Wu, J., and Black, W. C. (2011) Applying the pro-drug approach to afford highly bioavailable antagonists of $P2Y_{14}$. *Bioorg. Med. Chem. Lett. 21*, 4366−4368.

(15) Barrett, M. O., Sesma, J. I., Ball, C. B., Jayasekara, P. S., Jacobson, K. A., Lazarowski, E. R., and Harden, T. K. (2013) A selective high-affinity antagonist of the $P2Y_{14}$ receptor inhibits UDP-glucose−stimulated chemotaxis of human neutrophils. *Mol. Pharmacol. 84*, 41−49.

(16) Thirumurugan, P., Matosiuk, D., and Jozwiak, K. (2013) Click chemistry for drug development and diverse chemical−biology applications. *Chem. Rev. 113*, 4905−4979.

(17) Bach, P., Boström, J., Brickmann, K., van Giezen, J. J. J., Groneberg, R. D., Harvey, D. M., O'Sullivan, M., and Zetterberg, F. (2013) Synthesis, structure−property relationships and pharmacokinetic evaluation of ethyl 6-aminonicotinate sulfonylureas as antagonists of the $P2Y_{12}$ receptor. *Eur. J. Med. Chem. 65*, 360−375.

(18) Das, A., Zhou, Y., Ivanov, A. A., Carter, R. L., Harden, T. K., and Jacobson, K. A. (2009) Enhanced potency of nucleotide−dendrimer conjugates as agonists of the $P2Y_{14}$ receptor: multivalent effect in G protein-coupled receptor recognition. *Bioconjugate Chem. 20*, 1650−1659.

(19) Boger, D. L., McKie, J. A., Cai, H., Cacciari, B., and Baraldi, P. G. (1996) Synthesis and properties of substituted CBI analogs of cc-1065 and the duocarmycins incorporating the 7-methoxy-1,2,9,9a-tetrahydrocyclopropa[c]benz[e]indol-4-one (MCBI) alkylation subunit: magnitude of electronic effects on the functional reactivity. *J. Org. Chem. 61*, 1710−1729.

(20) Bélanger, G., Dupuis, M., and Larouche-Gauthier, R. (2012) Asymmetric total synthesis of (+)-virosine a via sequential nucleophilic cyclizations onto an activated formamide. *J. Org. Chem. 77*, 3215−3221.

(21) Flahaut, J., and Miginiac, P. (1978) Synthèse d'alcools acétyléniques par alkylation d'hydroxy-ω-alkynes-1. *Helv. Chim. Acta 61*, 2275−2285.

(22) Negishi, E., Boardman, L. D., Sawada, H., Bagheri, V., Stoll, A. T., Tour, J. M., and Rand, C. L. (1988) Metal promoted cyclization. 18. Novel cyclialkylation reactions of (ω-halo-1-alkenyl)metal derivatives. Synthetic scope and mechanism. *J. Am. Chem. Soc. 110*, 5383−5396.

(23) Sharma, S., and Oehlschlager, A. C. (1989) Scope and mechanism of stannylalumination of 1-alkynes. *J. Org. Chem. 54*, 5064−5073.

(24) Baker, M. V., Brown, D. H., Skelton, B. W., and White, A. H. (2000) Intramolecular hydroamination of 1,4,7-tri(pent-4′-yn-1′-yl)-1,4,7-triazacyclononane: formation of an azoniaspiro-[4.8]-tridecane. *Aust. J. Chem. 53*, 791−797.

(25) Mayrargue, J., Vayssière, M., and Miocque, M. (1985) A new synthesis of quinuclidinium derivatives. *Heterocycles 23*, 2173−2175.

(26) Vernekar, S. K. V., Hallaq, H. Y., Clarkson, G., Thompson, A. J., Silvestri, L., Lummis, S. C. R., and Lochner, M. (2010) Toward biophysical probes for the $5\text{-}HT_3$ receptor: structure−activity relationship study of granisetron derivatives. *J. Med. Chem. 53*, 2324−2328.

(27) Jayasekara, P. S., Barrett, M. O., Ball, C. B., Brown, K. A., Hammes, E., Balasubramanian, R., Harden, T. K., and Jacobson, K. A. (2014) 4-Alkyloxyimino derivatives of uridine-5′-triphosphate: distal modification of potent agonists as a strategy for molecular probes of $P2Y_2$, $P2Y_4$ and $P2Y_6$ receptors. *J. Med. Chem. 57*, 3874−3883.

(28) Cheng, Y. C., and Prusoff, W. H. (1973) Relationship between inhibition constant (K1) and concentration of inhibitor which causes 50% inhibition (I50) of an enzymatic-reaction. *Biochem. Pharmacol. 22*, 3099−3108.
(29) Kozma, E., Kumar, T. S., Federico, S., Phan, K., Balasubramanian, R., Gao, Z. G., Paoletta, S., Moro, S., Spalluto, G., and Jacobson, K. A. (2012) Novel fluorescent antagonist as a molecular probe in A_3 adenosine receptor binding assays using flow cytometry. *Biochem. Pharmacol. 83*, 1552−1561.
(30) Jayasekara, P. S., Barrett, M. O., Ball, C. B., Brown, K. A., Kozma, E., Costanzi, S., Squarcialupi, L., Balasubramanian, R., Maruoka, H., and Jacobson, K. A. (2013) 4-Alkyloxyimino-cytosine nucleotides: tethering approaches to molecular probes for the $P2Y_6$ receptor. *MedChemComm. 4*, 1156−1165.
(31) Abagyan, R. A., Orry, A., Raush, E., Budagyan, L., and Totrov, M. (2014) *ICM*, 3.8 ed., MolSoft LLC, La Jolla, CA.
(32) Abagyan, R., Batalov, S., Cardozo, T., Totrov, M., Webber, J., and Zhou, Y. (1997) Homology modeling with internal coordinate mechanics: deformation zone mapping and improvements of models via conformational search. *Proteins 1*, 29−37.
(33) Cardozo, T., Totrov, M., and Abagyan, R. (1995) Homology modeling by the ICM method. *Proteins 23*, 403−414.
(34) Totrov, M., and Abagyan, R. (1997) Flexible protein−ligand docking by global energy optimization in internal coordinates. *Proteins 1*, 215−220.
(35) Fricks, I. P., Carter, R. L., Lazarowski, E. R., and Harden, T. K. (2009) G_i-dependent cell signaling responses of the human $P2Y_{14}$ receptor in model cell systems. *J. Pharmacol. Exp. Ther. 330*, 162−168.
(36) Salomon, Y., Londos, C., and Rodbell, M. (1974) A highly sensitive adenylate cyclase assay. *Anal. Biochem. 58*, 541−548.
(37) Harden, T. K., Scheer, A. G., and Smith, M. M. (1982) Differential modification of the interaction of cardiac muscarinic cholinergic and beta-adrenergic receptors with a guanine nucleotide binding components. *Mol. Pharmacol. 21*, 570−580.
(38) Jacobson, K. A., Jayasekara, M. P. S., and Costanzi, S. (2012) Molecular structure of P2Y receptors: mutagenesis, modeling, and chemical probes. *Wiley Interdiscip. Rev.: Membr. Transp. Signaling 1*, 815−827.
(39) Bhowmick, N., Narayan, P., and Puett, D. (2012) The endothelin subtype A receptor undergoes agonist- and antagonist-mediated internalization in the absence of signaling. *Endocrinology 139*, 3185−3192.
(40) Ciruela, F., Jacobson, K. A., and Fernández-Dueñas, V. (2014) Portraying G protein-coupled receptors with fluorescent ligands. *ACS Chem. Biol. 9*, 1918−1928.